Biophysical Journal Volume 89 October 2005 2750–2758

Substrate-Supported Phospholipid Membranes Studied by Surface Plasmon Resonance and Surface Plasmon Fluorescence Spectroscopy

Keiko Tawa and Kenichi Morigaki

Research Institute for Cell Engineering, National Institute of Advanced Industrial Science and Technology (AIST), Ikeda, Osaka 563-8577, Japan

ABSTRACT Substrate-supported planar lipid bilayer membranes are attractive model cellular membranes for biotechnological applications such as biochips and sensors. However, reliable fabrication of the lipid membranes on solid surfaces still poses significant technological challenges. In this study, simultaneous surface plasmon resonance (SPR) and surface plasmon fluorescence spectroscopy (SPFS) measurements were applied to the monitoring of adsorption and subsequent reorganization of phospholipid vesicles on solid substrates. The fluorescence intensity of SPFS depends very sensitively on the distance between the gold substrate and the fluorophore because of the excitation energy transfer to gold. By utilizing this distance dependency, we could obtain information about the topography of the adsorbed membranes: Adsorbed vesicles could be clearly distinguished from planar bilayers due to the high fluorescence intensity. SPSF can also incorporate various analytical techniques to evaluate the physicochemical properties of the adsorbed membranes. As an example, we demonstrated that the lateral mobility of lipid molecules could be estimated by observing the recovery of fluorescence after photobleaching. Combined with the film thickness information obtained by SPR, SPR-SPFS proved to be a highly informative technique to monitor the lipid membrane assembly processes on solid substrates.

INTRODUCTION

Substrate-supported planar lipid bilayers (termed simply planar bilayers in the following) represent versatile model membrane systems for fundamental studies of the biological membrane as well as for biomedical applications (1). Planar bilayers have been used to study cell-cell recognition in the immune system (2–4), cell adhesion (5,6), and reconstitution of membrane proteins (7–11). Planar bilayers are usually prepared by two different methods: 1), consecutive transfer of lipid monolayers from aqueous surfaces (the Langmuir-Blodgett/Langmuir-Schaefer method), and 2), the adsorption and reorganization of lipid vesicles on the substrate surface (the vesicle fusion method) (2,12). The latter method is increasingly becoming popular, primarily because it is a simple self-assembly process. However, reliable and routine formation of planar bilayers via vesicle fusion still remains an experimental challenge for various combinations of substrates and lipids. For reliable production of planar bilayers, development of analytical tools to monitor the vesicle fusion process is important. To date, various analytical techniques have been applied to the monitoring of the vesicle fusion process, including light microscopy-based techniques (13,14), impedance spectroscopy (15), surface plasmon resonance (SPR) (16,17), ellipsometry (18), quartz crystal microbalance with dissipation monitoring (QCM-D) (19–21), and atomic force microscopy (AFM) (21–24). Although these analytical tools contributed significantly to the fundamental understanding of the vesicle fusion process, the subtle interplay of various factors that determine the self-assembly process and the physicochemical properties of thus formed membranes remain rather poorly understood.

Recently, surface plasmon fluorescence spectroscopy (SPFS) was introduced as a technique that offers higher detection limits and higher sensitivity than the SPR and QCM-D methods (25,26). SPFS is fluorescence spectroscopy that uses the excitation by an evanescent field amplified at the metal-dielectric interface, i.e., a surface plasmon field. It is highly surface specific and extremely sensitive owing to the surface plasmon field, which can be enhanced ~20 times compared with the field of total internal reflection (27). For example, point mutant detection between oligonucleotides (15 basepairs) in a dilute surface is difficult to observe by SPR quantitatively, whereas a quantitative analysis of the association (hybridization) and dissociation process was possible by SPFS using target oligonucleotide chemically labeled with a fluorescent molecule (28).

In this article we present the application of simultaneous SPR-SPFS measurements to study the formation of biomimetic lipid membranes on solid surfaces. Adsorption and transformation of phospholipid vesicles into planar bilayers were observed on gold substrates covered either by a self-assembled monolayer (SAM) of thiols or by a silica layer of defined thickness (Fig. 1). In the combined SPR-SPFS analysis, the thickness of the adsorbed lipid materials can be determined in the subnanometer precision by SPR, whereas information related to the topography and physicochemical properties of the membrane can be provided by SPFS. We demonstrate the capacity of SPR-SPFS to distinguish the type of adsorbed membranes (whether vesicles or planar bilayers are adsorbed) by using the distance-dependent fluorescence quenching by the gold substrate. Furthermore, introduction of fluorescence allows the application of various fluorescence-based analytical techniques. As an example, SPFS was applied to estimate the lateral mobility of membrane-associated molecules by monitoring the recovery of fluorescence after photobleaching.

Submitted May 2, 2005, and accepted for publication July 14, 2005.

Address reprint requests to Keiko Tawa, E-mail: tawa-keiko@aist.go.jp; or Kenichi Morigaki, E-Mail: morigaki-kenichi@aist.go.jp.

0006-3495/05/10/2750/09 $2.00

doi: 10.1529/biophysj.105.065482

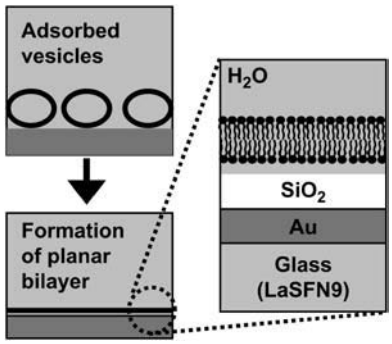

FIGURE 1 Scheme of the vesicle fusion process. The adsorbed vesicles either transform into a planar bilayer or remain intact. The right side depicts the silica-coated substrate used in this study.

Finally, we compare SPR-SPFS with other analytical methods to discuss its advantages and current limitations.

MATERIALS AND METHODS

Materials

Phosphatidylcholine from egg yolk (egg-PC) was purchased from Avanti Polar Lipids (Alabaster, AL). 1,1′-dioctadecyl-3,3,3′,3′-tetramethylindodicarbocyanine perchlorate (DiD; excitation/emission: 644 nm/665 nm, extinction coefficient: 260,000) was purchased from Molecular Probes (Eugene, OR). Thiols, i.e., thioglycolic acid ($HSCH_2COOH$), 2-mercaptoethylamine ($HS(CH_2)_2NH_2$), and 1-dodecanethiol ($HS(CH_2)_{11}CH_3$), were purchased from Aldrich (St. Louis, MO). All other chemicals were purchased as the reagent grade and used without further purification. Glass substrates ($25 \times 25 \times 1.5$ mm) with a high refractive index (LaSFN9: $\varepsilon' = 3.4069$ at $\lambda = 632.8$ nm) were obtained from Hellma Optik (Jena, Germany). Gold (Au), chromium (Cr), and silica (SiO_2) targets for the sputtering were obtained from Furuuchi Chemical (Tokyo, Japan).

Substrates preparation

LaSFN9 glass substrates were cleaned by sonicating in a 1% Hellmanex (Hellma, Müllheim, Germany) solution for 20 min and rinsing extensively with fresh Milli-Q water. Finally, they were completely dried under airflow.

Either of the following surface configurations was constructed on the LaSFN9 substrate: 1), an Au thin layer covered with a SAM of thiols, or 2), an Au thin layer covered with a SiO_2 overlayer (with an adhesion layer of Cr). Au, Cr, and SiO_2 coating was prepared by sputtering. An Au thin film was deposited by a direct current (DC)-magnetron sputtering of 100 W onto LaSFN9 glass substrates in an Ar gas of 8 Pa in pressure (SINKO SEIKI SCV-430, Nagano, Japan). The sputtering time was ~1 min so that a gold layer thickness could be set to 48 ± 5 nm. The SiO_2 substrates were prepared by the following two steps using a different sputtering machine (Rikensya RSP-4-RF5/DC5, Osaka, Japan). First, a Cr layer of <1-nm thick was deposited by the DC sputtering with a power of 5 W at room temperature onto the Au surface in an Ar gas of 0.1 Pa. Subsequently, a SiO_2 layer of 3–80-nm thick was deposited onto the Cr layer by an RF-magnetron sputtering with a power of 100 W at room temperature in an Ar gas of 0.1 Pa.

SAMs were formed from an ethanol solution (concentration: 1–5 mM) in situ in the sample cell built in the SPR-SPFS setup (vide infra). The SAM formation was monitored by SPR.

Vesicle preparation

Vesicle suspensions of 1 mM egg-PC containing a trace amount of DiD fluorescence marker (0.01 M phosphate buffer with 0.15 M NaCl (pH 6.6)) were prepared by the following protocol. Lipids were mixed in a chloroform solution and the solvent was evaporated by a stream of nitrogen and vacuum, and the lipids were allowed to hydrate in buffer. The resulting multilamellar vesicles were put through five freeze-thaw cycles and then extruded through a polycarbonate filter with pores of 50 nm diameter (LiposoFast, Avestin, Ottawa, Canada).

SPR-SPFS measurements

The details of the SPFS setup are described in previous articles (26,28). Briefly, the setup is based on essential modules of a ''normal'' surface plasmon spectrometer as shown in Fig. 2. A He-Ne laser operating at 632.8 nm passes an optical chopper (used also as the reference for the lock-in amplifier) and two polarizers for intensity and polarization control. By using a $\theta-2\theta$ goniometer, the light reflected at the substrate covered with a thin gold layer is monitored by a photo diode. Here, the diameter size of the laser spot was ~1 mm. Any change of the interfacial architecture, e.g., induced by adsorption or desorption processes, can be quantified by evaluating the resulting shift of the SPR spectra. As discussed in the previous article (26), the optical field which is strongly enhanced at the SPR angle can be used to excite fluorescence molecules attached to the surface-bound analyte. The angular characteristic of the fluorescence intensity then follows the angular dependence of the optical field at the interface. Compared with the intensity enhancement for total internal reflection (~4 times that of the incident light) at the critical angle, the enhancement for SPR can reach up to 20–30 times higher. Fluorescent molecules that are within the evanescent field, which decays normal to the interface with a penetration depth of $Lz = 150$ nm, can be excited by this surface plasmon mode. The emission is monitored by a photomultiplier (after passing through an appropriate lens, 10%-ND filter, and a narrow band interference filter, $\lambda = 670 \pm 5$ nm) mounted to the goniometer part that rotates with θ, as does the coupling prism (Fig. 2). The time-dependent fluorescence spectra were also observed by SPFS.

The employed sample cell is made of teflon and contains in- and outlets for the solution exchanges. Two sides of the cell are sealed via a Viton O-ring against a quartz plate and an Au-coated high refractive glass slide (LaSFN9), which is index matched to the prism, respectively. The diameter of a substrate applicable to the formation of a planar lipid bilayer is 6.0 mm, i.e., large enough compared with the observation area (the size of the laser spot). All solutions used in this study were prepared using a phosphate buffer (0.01 M) with additional NaCl (0.15 M) at pH = 6.6. All measurements were performed at room temperature (22°C −23°C).

For the measurement of fluorescence recovery after photobleaching (FRAP), the same SPFS setup was used. The incident light was focused to a smaller spot at the center of the illumination area used for other SPR-SPSF measurements. Before photobleaching, the initial fluorescence intensity was measured by opening the shutter for 1 s every 10 min. The intensity was attenuated to 10% with an ND filter inserted in front of the prism. Photobleaching was performed by keeping the shutter open for 2 min without the ND filter

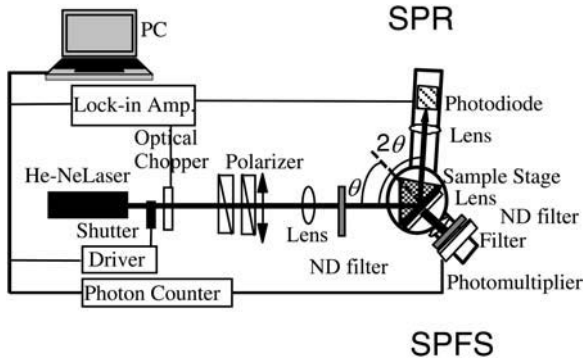

FIGURE 2 Schematic diagram of the SPR-SPFS setup.

(100% power). After photobleaching, the recovery of fluorescence was observed by opening the shutter again for 1 s every 10 min with the ND filter inserted in front of the prism.

RESULTS AND DISCUSSION

Adsorption and transformation of phospholipid vesicles observed by SPR-SPFS

We first describe typical SPR-SPFS observations made during the vesicle fusion process. Fig. 3 shows SPR-SPFS spectra and kinetic measurements for the adsorption of phospholipid vesicles on a gold substrate modified with a monolayer of carboxylate-terminated alkanethiol (COOH). As egg-PC vesicles containing DiD marker (10^{-4} mol/mol) adsorbed onto the substrate surface, the SPR dip shifted to a larger angle and a fluorescence peak appeared in the same angle region (Fig. 3 *A*). The SPR curve was fitted to the theoretical model based on Fresnel's equation to obtain the adsorbed film thickness, assuming the refractive index of phospholipid bilayers to be 1.49 (29,30). (Software called WINSPALL was used for the fitting. It is based on the Fresnel equations and the matrix formalism. WINSPALL was developed in Prof. Wolfgang Knoll's group at the Max-Planck-Institute for Polymer Research (Mainz, Germany) and is publicly available for the analysis of SPR (http://www.mpip-mainz.mpg.de/documents/akkn/index.html).) The obtained thickness and fluorescence intensity were plotted versus the elapsed time (Fig. 3 *B*). (In this study, the information obtained from SPR-SPFS measurement was averaged within the area corresponding to the laser spot with the diameter of ~1 mm as described in the Materials and Methods section. The adsorbed membrane is assumed to be homogeneous within the area.) The adsorbed film thickness reached a plateau value of ~8.0 nm within 400 s and increased only slightly afterwards, whereas the fluorescence intensity decreased gradually after reaching the maximum. The vesicle suspension was exchanged with a buffer solution after incubation of ~90 min. Both the film thickness and fluorescence intensity remained unchanged. As the cell was further rinsed with Milli-Q water, we observed a drastic decrease of the film thickness and fluorescence intensity (Fig. 3, *A* and *B*). The obtained final film thickness was 3.7 nm, which corresponds to the thickness of a phospholipid bilayer. (Milli-Q water and buffer solution have different refractive indices. This difference was incorporated in the SPR curve fitting to evaluate the adsorbed layer thickness.) On the other hand, the SPR-induced fluorescence practically diminished due to the excitation energy transfer to the gold substrate, which is an indication for the formation of a planar bilayer, as described in detail in the following section.

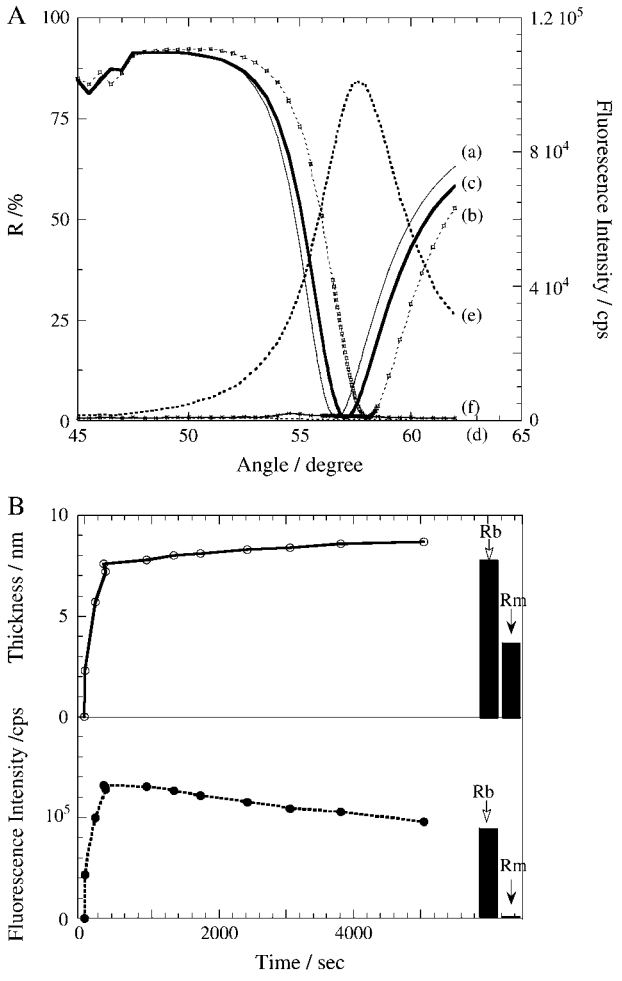

FIGURE 3 Vesicle fusion process on a COOH surface monitored by SPR-SPFS. (*A*) SPR (*solid lines*) and SPFS (*broken lines*) spectra before adding egg-PC vesicles (*a* and *d*), after rinsing with buffer solution (*b* and *e*), and after rinsing with Milli-Q water (*c* and *f*), respectively. (*B*) The time evolution of the lipid layer thickness observed by SPR (*upper frame*) and the fluorescence intensity observed by SPFS (*bottom frame*) in the vesicle fusion process. The bars Rb and Rm indicate the values after rinsing with buffer and Milli-Q water, respectively.

Distance-dependent energy transfer from the adsorbed film to the gold substrate

Nonradiative energy transfer from an excited molecule to the nearby gold substrate is an effective decay channel for the excited molecule. The efficiency of excitation energy transfer is distance dependent, and its purposeful use plays a critical role in these SPR-SPFS measurements. The distance-dependent energy transfer rate from a donor molecule to a planar surface has been previously discussed using the so-called CPS model (after R. R. Chance, A. Prock, and R. Silbey) (31). Unlike the Förster transfer between dipoles of molecules, which has the energy transfer rate inversely proportional to the sixth power of the distance between donor-acceptor molecules, the energy transfer rate from a donor molecule to the planar metal substrate decays with the third power of the distance (vide infra) (32,33).

To assess the distance dependency of the energy transfer (quenching), we have fabricated gold substrates covered with

silica of varied thickness and observed the fluorescence intensity from absorbed egg-PC/DiD bilayers. Fig. 4 shows the SPR-SPFS spectra and the time evolution of layer thickness and fluorescence intensity obtained during the vesicle fusion process. The thickness of the SiO_2 layer prepared on Au substrate was 3.3 nm in Fig. 4, *A* and *C*, and 19 nm in Fig. 4, *B* and *D*, respectively. After rinsing with buffer solution and Milli-Q water, the remaining film thickness was 4.0 nm in both cases, indicating the adsorption of a planar bilayer membrane. The fluorescence intensity decreased practically to zero by rinsing with Milli-Q water in the case of Fig. 4, *A* and *C*, whereas it decreased only slightly in the case of Fig. 4, *B* and *D*. The different attenuation behaviors of fluorescence intensity shown in these two samples result from different efficiency of energy transfer from excited DiD molecules in the bilayer to the gold layer. The thickness of the dielectric layer that separated the bilayer and gold substrate was much thinner in the former case, enabling more efficient energy transfer. Fig. 5 shows a plot of the fluorescence intensity and film thickness of adsorbed egg-PC bilayers as a function of the SiO_2 layer thickness. In all data points the adsorption behaviors of the vesicles were monitored by SPR and SPFS simultaneously. Formation of planar bilayers was postulated from the SPR data in which the film thickness was constantly ~4.0 nm. On the other hand, the fluorescence intensity increased up to ~50 nm and decayed gradually for larger distances.

The observed distance dependency can be explained by the quenching effect and the power attenuation of the evanescent field. The intensity of fluorescence excited by the surface plasmon field at a distance of d_1 from the gold surface, $F(d_1)$, can be described as

$$F(d_1)/F_0 = I_{ex}(d_1)/I_0 * \Phi(d_1)/\Phi_0, \quad (1)$$

which is normalized to the theoretical fluorescence intensity at the gold surface ($d_1 = 0$) under the assumption that no quenching occurs, F_0. $I_{ex}(d_1)$ and I_0 are the optical power of excitation at the distance of d_1 and on the gold surface, respectively. $\Phi(d_1)$ and Φ_0 are the fluorescence quantum yield with and without considering d_1-dependent energy transfer to gold, respectively. $I_{ex}(d_1)$ can be expressed using distance-dependent attenuation of the evanescent field as

$$I_{ex}(d_1) = I_0 * \exp(-2\pi/\lambda_{ex} * n_1 * d_1 * ((n_0/n_1)^2 * (\sin\theta)^2 - 1)), \quad (2)$$

in which λ_{ex}, n_0, and θ are the wavelength of incident light, the refractive index of prism (1.85), and the observed angle, respectively. n_1 and d_1 correspond to the refractive index and the thickness of the dielectric layer that is separating the fluorophore from the gold surface.

On the other hand, Φ can be generally described as below using three rate constants corresponding to the radiative (fluorescence) rate (k_r), the nonradiative rate (k_{nr}), and the energy transfer rate (k_{ET}) from excited molecules.

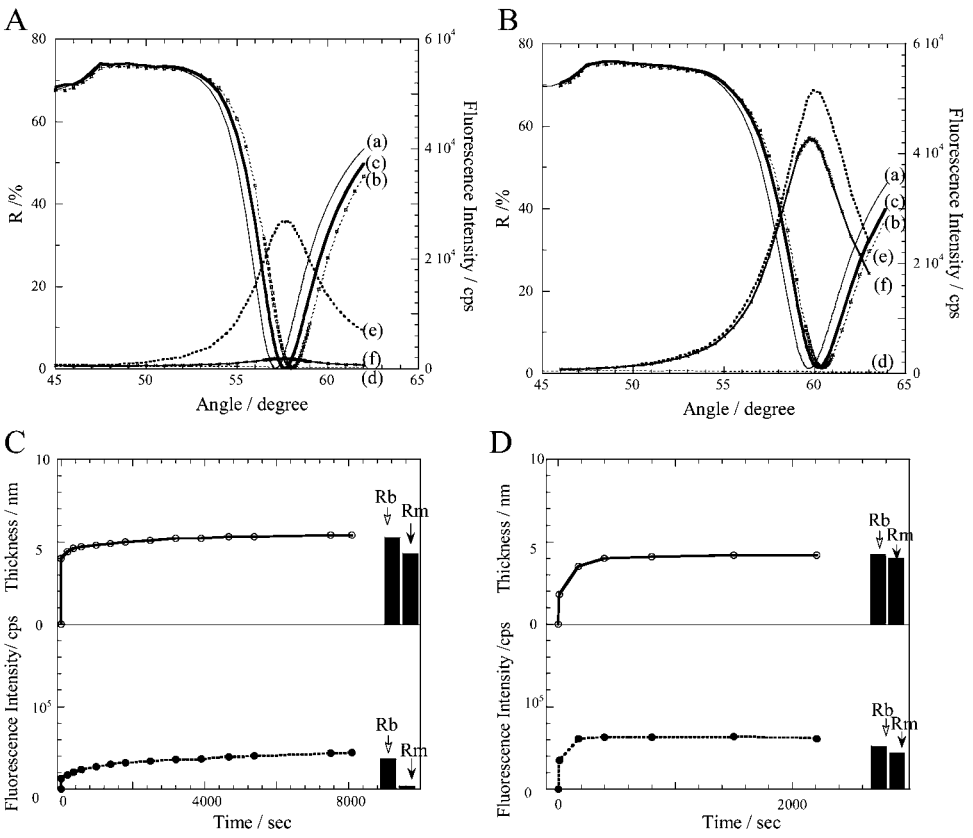

FIGURE 4 Vesicle fusion process on a SiO_2 surface monitored by SPR-SPFS. SPR (*solid lines*) and SPFS (*broken lines*) spectra before adding egg-PC vesicles (*a* and *d*)), after rinsing with buffer (*b* and *e*), and after rinsing with Milli-Q water (*c* and *f*), respectively, (*A*) at SiO_2 (3.3 nm) surface and (*B*) at SiO_2 (19 nm) surface. The time evolution of the lipid layer thickness observed by SPR (*upper frame*) and the fluorescence intensity observed by SPFS (*bottom frame*) in the vesicle fusion process (*C*) at SiO_2 (3.3 nm) surface and (*D*) at SiO_2 (19 nm) surface. The bars Rb and Rm are the same as in Fig. 3.

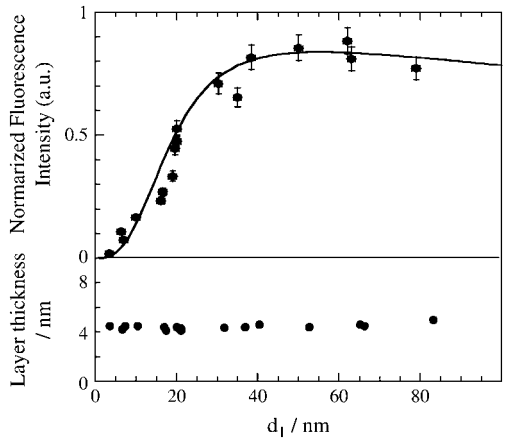

FIGURE 5 SiO_2 thickness dependence of the fluorescence intensity observed by SPFS and the theoretical curve for fluorescence quenched by the Förster mechanism (*upper frame*). The lipid layer thicknesses evaluated by SPR for each SiO_2 interface are also shown in the bottom frame.

$$\Phi = k_r/(k_r + k_{nr} + k_{ET}). \quad (3)$$

Therefore, Φ/Φ_0 can be described as

$$\Phi/\Phi_0 = 1/(1 + (k_{ET}/(k_r + k_{nr}))) = 1/(1 + (\hat{b}_{ET})), \quad (4)$$

where $\hat{b}_{ET}$ is defined by $k_{ET}/k_r + k_{nr}$. As mentioned above, the distance dependence of the energy transfer rate from a donor molecule to the planar metal surface has been described most quantitatively using the CPS model. Under the conditions that $\hat{d}_1$ ($= \nu_1 d_1$) $\ll 1$, d_2 is large, and $d_2/d_1 \geq 1$, where d_2 is the gold layer thickness and ν_1 is defined by $n_1 2\pi/\lambda_{em}$ (λ_{em}: wavelength of emission), the normalized energy transfer rate, $\hat{b}_{ET}$, can be theoretically expressed (along the lines of Förster transfer theory) by

$$\hat{b}_{ET} = p * \Phi_0/4 * (\hat{d}_1)^{-3} * Im((\varepsilon_2(\omega) - \varepsilon_1)/(\varepsilon_2(\omega) + \varepsilon_1)) = \beta * (d_1)^{-3}, \quad (5)$$

in which p and ε express the orientation factor for transition moment of fluorescent molecules and the frequency-dependent complex dielectric constant composed of real (ε') and imaginary (ε'') parts, respectively. The subscripts 1 and 2 denote the dielectric and gold layers, respectively. Depending on whether the transition moment aligns to the direction parallel or perpendicular to the substrate surface, the value of p can be set as 3/4 or 3/2, respectively. The transition moment of fluorescent molecule, DiD, used in this study is considered to tilt at ~75–80° to the metal surface normal (34), i.e., to be almost parallel to the surface (35,36). Therefore, the value of p was set to 0.8 in this study. The fluorescence quantum yield of DiD could be assumed to be near 1.0 by referring to the previous reports (37,38). Under the currently used experimental conditions (gold layer thickness (d_2) = 48 ± 5 nm, refractive index of SiO_2 (n_1) = 1.45, and fluorescence wavelength (λ_{em}) = 670 nm), Eq. 5 is considered to be valid for $d_1 < \sim 70$ nm. As found from Eq. 5, $\hat{b}_{ET}$ can be expressed by the product of the constant value, β, and the reciprocal of the third power of d_1. By introducing Eqs. 2, 4, and 5 to Eq. 1, $F(d_1)/F_0$ is derived to be

$$F(d_1)/F_0 = \exp(-2\pi/\lambda_{ex} * n_1 * d_1 * ((n_0/n_1)^2 * (\sin\theta)^2 - 1)) * 1/(1 + \beta * (d_1)^{-3}). \quad (6)$$

For a small d_1, the second term (quenching) dominates the obtained $F(d_1)/F_0$ value, whereas the first exponential term (decay of the evanescent wave) becomes determinant for a large d_1. We have simulated the fluorescence intensity from an adsorbed planar bilayer assuming that equal amounts of DiD molecules are distributed to each side of the bilayer. As an approximation, the vertical displacement of fluorophore in the two monolayers was assumed to be 4 nm, i.e., that DiD molecules existed at d_1 and $d_1 + 4$ nm, and the same refractive index as SiO_2 (1.45) was used for the lipid layer. Furthermore, the thickness of the aqueous layer which is supposed to exist between the lipid layer and the substrate was neglected. The simulation curve depicted in Fig. 5 was obtained by using $\varepsilon_2(\omega) = -10.0 + 1.45i$, which is appropriate as the complex dielectric constant of gold at the wavelength of 670 nm. The simulation curve agrees significantly well to the experimental results, validating the adequacy of the CPS model for the excitation energy transfer between the adsorbed membrane and the underlying substrate. This result in turn shows that the separation between the adsorbed lipid membrane and the gold substrate (d_1) can be deduced from the fluorescence intensity observed by the SPSF measurements.

Interface-dependent adsorption and transformation of phospholipid bilayers

The distance-dependent fluorescence intensity in the SPFS measurements gives information concerning the separation of the adsorbed lipid films from the gold substrate. Bilayers in vesicles generally have a larger separation compared with planar bilayers. Accordingly, for a given amount of lipid film adsorbed, which can be determined by SPR, they have much higher fluorescence intensities detected by SPFS compared with planar bilayers. Therefore, basically it is possible to distinguish whether vesicles are adsorbed on the surface or are transformed into a planar bilayer. For example, the difference is evident in Fig. 3. After the incubation with egg-PC/DiD vesicles, the substrate surface was successively rinsed with buffer solution and Milli-Q water. Rinsing with the buffer solution hardly changed the fluorescence intensity, whereas rinsing with Milli-Q water drastically reduced it. At the same time, the film thickness obtained from SPR was reduced from 7.8 nm to 3.7 nm. The high fluorescence intensity after the buffer rinsing indicates that there was still a considerable amount of excess lipid material adsorbed as vesicles. Rinsing with Milli-Q water removed these vesicles,

leaving a planar bilayer on the substrate. (We currently do not have a mechanistic explanation for the effectiveness of the Milli-Q water rinsing, although it has been reported that rinsing with a dilute NaOH solution effectively removes loosely absorbed phospholipid vesicles from the surface by electrostatic repulsion (17).)

Table 1 summarizes the SPR-SPFS data for the vesicle fusion experiments on various substrates. For SAM surfaces, the interface is very close to the gold substrate and formation of planar membranes (either monolayer or bilayer) is characterized by a very low fluorescence intensity due to the effective quenching and an appropriate layer thickness. Therefore, the adsorbed lipid films on COOH and CH_3 surfaces after Milli-Q water rinsing are concluded to be a single sheet of planar bilayer and monolayer, respectively. (Vesicle fusion on hydrophilic surfaces was less reproducible compared with that on hydrophobic surfaces. Whether vesicles remain adsorbed on the substrate was very much dependent on individual samples.) On the other hand, judging from the high fluorescence intensity, there are adsorbed vesicles on the NH_2 surface. The adsorbed vesicles may be trapped to the surface by electrostatic interactions. The fluorescence intensity even increased after the Milli-Q water rinsing, indicating that the shape of the vesicles changed. It should be noted that although high fluorescence intensity is a clear indication of adsorbed vesicles, it does not exclude the possibility that a planar bilayer also exists on the substrate.

For silica surfaces, the adsorption behaviors were more straightforward. It is well established that PC vesicles tend to form a planar bilayer on hydrophilic silica surfaces (19). The film thickness after Milli-Q water rinsing was ~4.0 nm, as determined by SPR, corroborating the planar bilayer formation. On the other hand, the fluorescence intensities increased with the thickness of the silica layer that separated the adsorbed film from the gold layer, as discussed in the previous section.

To obtain further insight into the vesicle adsorption and transformation process, we have plotted the fluorescence intensity versus the film thickness observed during the vesicle fusion process (Fig. 6). Fig. 6 *A* shows the fusion process on the SAM surfaces. Three kinds of surfaces were compared, i.e., a hydrophobic CH_3 surface, a negatively charged COOH surface, and a positively charged NH_2 surface. For all three surfaces, the fluorescence increased linearly with the lipid layer thickness in the early stage of the incubation with vesicle suspensions. The slopes were nearly the same. Since the adsorption occurred at an interface that is located very close to the gold substrate (<1.5 nm), the observed fluorescence is supposed to have arisen mostly from adsorbed vesicles regardless of the kind of SAMs. The thickness exceeded the expected values for planar bilayers and monolayers, and the fluorescence intensities started to decrease slightly above the thickness of ~7 nm in the case of hydrophilic surfaces. The reduction may be because of the topographical changes of the adsorbed vesicles (either flattening of vesicles or transformation into planar bilayers). The incubation was terminated at the point depicted with open symbols. The changes that followed the rinsing processes with buffer and Milli-Q water are indicated as crossed and solid symbols, respectively. (These changes are also shown in Table 1.) As described previously, fluorescence from the adsorbed films diminished to nearly zero in the case of CH_3 and COOH surfaces, suggesting the formation of planar membranes.

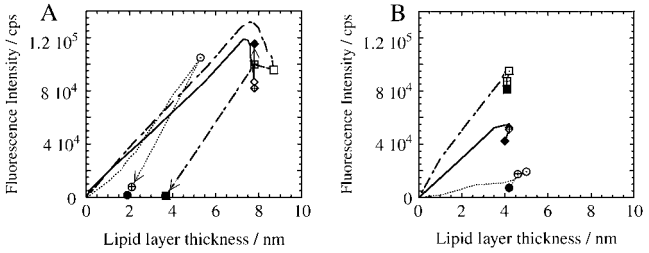

FIGURE 6 Plot of fluorescence intensity versus adsorbed lipid film thickness during the vesicle fusion process. (*A*) At the SAM surfaces with COOH (*broken line*, □), CH_3 (*dotted line*, ○), and NH_2 (*solid line*, ◇) terminal groups, (*B*) at the surface of SiO_2 with the thickness of 6.9 nm (*dotted line*, ○), 19.6 nm (*solid line*, ◇), and 50.0 nm (*broken line*, □). The open symbols indicate the time point when the incubation with vesicle suspensions was terminated. The incubation time was 90 min, 125 min, 95 min, and 40 min for COOH, CH_3, NH_2, and SiO_2 surfaces, respectively. After incubation, the cell was successively rinsed with buffer solution and Milli-Q water. The crossed symbols and the solid symbols correspond to the data points after the rinse with buffer and Milli-Q water, respectively.

Fig. 6 *B* shows the fusion processes on the surface of SiO_2 layers with the thickness of 6.9, 19.6, and 50.0 nm. In either case, the fluorescence intensity increased linearly with the lipid layer thickness. The slope was larger for samples with a thicker SiO_2 layer, as expected from the quenching effect. The rinsing with Milli-Q water caused only a slight decrease in the fluorescence, indicating that there are not many excessive adsorbed vesicles. The linear increase of fluorescence with respect to the thickness also indicates that the amount of transiently adsorbed vesicles during the vesicle fusion process is rather small in the timescale of current SPR-SPFS measurements. For the vesicle fusion of PC on silica, QCM-D and AFM studies have demonstrated the presence of nonruptured vesicles accumulated on the surface before the

TABLE 1 Lipid layer thickness and fluorescence intensity on the various interfaces after rinsing with buffer and Milli-Q water

Interface	Layer thickness/nm		Fluorescence intensity/cps	
	Buffer rinse	Milli-Q rinse	Buffer rinse	Milli-Q rinse
COOH	7.8	3.7	105,000	1,400
NH_2	7.8	7.8	81,500	114,500
CH_3	2.1	1.9	7,600	1,900
SiO_2 d_1= 3.3 nm	5.2	4.2	27,000	1,600
SiO_2 6.3 nm	4.0	3.9	12,200	10,000
SiO_2 20.0 nm	3.9	3.8	51,600	44,000
SiO_2 50.0 nm	4.1	4.1	87,000	81,000

formation of planar bilayers. A lower limit of the adsorbed vesicle amount (critical vesicle concentration) was proposed as a necessary condition for the transition from vesicles to planar bilayer. Such accumulation of vesicles should have resulted in a temporal rise in fluorescence. Absence of this observation in Fig. 6 *B* may indicate that adsorbed vesicles transformed rather directly into a planar bilayer without accumulation on the substrate surface. (It is known that under some conditions lipid vesicles can also transform directly into planar discs upon adsorption onto the substrate.) However, the real reason for the different observations in previous QCM-D/AFM studies and current SPR-SPSF measurements is currently not clear. Further experiments are necessary for more detailed analysis of the fusion mechanism.

FRAP of the planar phospholipid bilayer

In biological membranes, lateral mobility of membrane-associated molecules is essentially important for their functions. Therefore, lateral mobility has often been regarded as a criterion for the successful reconstitution of artificial model membranes on solid supports. For the assessment of this property, the FRAP technique has been widely used, which monitors the recovery of fluorescence in the locally photobleached spot by an attenuated illumination. To evaluate the lateral diffusion of lipid molecules in the planar bilayers, FRAP was in situ measured using the same SPR-SPFS as the observation of the vesicle fusion process. A typical recovery profile is shown in Fig. 7. We have locally photobleached the fluorophore (DiD) in a planar egg-PC bilayer formed on a gold substrate covered with a 20-nm-thick silica layer with an intense plasmon excitation light. The fluorescence recovery was subsequently monitored by an attenuated plasmon excitation. The recovery of fluorescence clearly showed that the lipid bilayer membrane was fluid and continuous over a long distance. The diffusion constant of DiD in the bilayer was estimated to be $0.9 \pm 0.5\ \mu m^2/s$ by fitting the experimental data to the diffusion equation originally proposed by Axelrod et al. (39) and modified by Soumpasis (40). The observed diffusion was rather slow for a typical phospholipid bilayer, and the uncertainty was also large. It is primarily due to the fact that we used a rather large, elliptic illumination area ($\sim 250\ \mu m \times 500\ \mu m$) and observed the recovery for a prolonged period of time. Though these configurations are certainly not ideal for quantitative determination of the diffusion coefficients, current results demonstrate that the assessment of the membrane lateral mobility by the SPR-SPFS measurements is feasible.

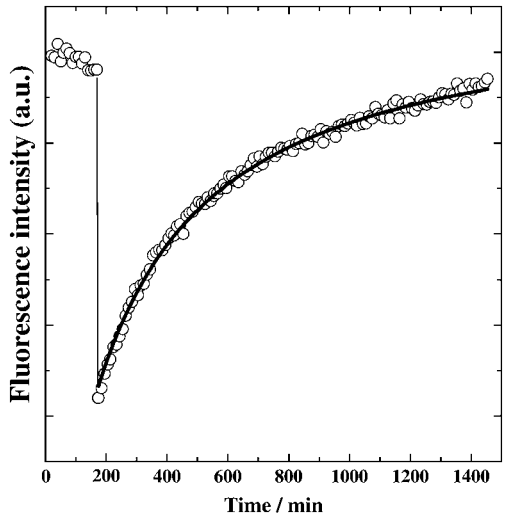

FIGURE 7 FRAP profile of an adsorbed egg-PC/DiD bilayer on an SiO_2 substrate (thickness 20 nm). The solid line is a fit to the theoretical model by Axelrod et al. (39) and Soumpasis (40).

Comparison with other analytical techniques

Simultaneous SPR-SPFS analysis has various unique advantages for evaluating the formation of biomimetic membranes on solid substrates. One of the most significant features is the ability of SPFS to give information related to the topography of the membrane, i.e., separation from the substrate surface. Conventional SPR can determine the adsorbed film thickness, but it is not possible to acquire information on the topography of adsorbed membranes. As described above, by using SPR-SPFS we can distinguish unambiguously whether vesicles or planar bilayers are adsorbed on the substrate surface. We showed by the SPFS data that vesicles remain adsorbed on some substrate surfaces even after rinsing with buffer solution or Milli-Q water. It would be impossible to distinguish adsorbed vesicles from planar bilayers solely from SPR measurements, partially because the optical constants of the membrane are also variable. It should be noted, however, that the presence of adsorbed vesicles does not necessarily exclude the possibility that planar bilayers also exist. It is currently not possible to quantitatively evaluate the amount of coadsorbed vesicles and planar bilayers. One may be able to obtain information by carefully analyzing the relation between the measured thickness and fluorescence intensity, as shown in Fig. 6. It is a difficult task, however, because various factors such as shape changes of adsorbed vesicles can also affect the fluorescence intensity.

QCM-D and AFM are currently widely applied to the monitoring of vesicle fusion processes (21,41). They can also determine whether vesicles are transformed into planar bilayers and have provided important insights into the mechanism of the planar membrane formation. SPR-SPFS has potentially the same applicability as these methods in terms of observing the membrane formation process in situ and giving real-time information related to the state of the formed membrane. QCM-D measures the mass of adsorbed vesicles including trapped water molecules, whereas SPR-SPFS measures the fluorescence from membrane-bound chromophores. On the other hand, AFM can image individual

adsorbed vesicles or planar bilayer disks formed by the rupture of vesicles. A systematic comparison of the results obtained by SPR-SPSF with these techniques should give new insights into the vesicle adsorption and transformation processes at the solid-liquid interface. Mica has often been used as substrates for the AFM measurements. A recent comparative study by the QCM-D and AFM techniques suggested that vesicle fusion behaviors on mica and silica are considerably different (41). Application of mica substrates for SPSF measurements might be technically difficult because a thin mica layer with a defined thickness has to be attached on the gold substrate. On the other hand, it is possible to deposit oxide layers of various compositions by the sputtering process (i.e., doping of silica, deposition of titanium oxide, etc.). In recent years, there have been some studies which combined SPR with QCM-D, resolving the amount of adsorbed vesicles and planar bilayers during the vesicle fusion process (42,43). Since SPR-SPSF provides information more directly related to the topography of adsorbed membranes, its application with QCM-D should vastly enhance the quality of acquired information.

Another significant feature of SPR-SPFS is the fact that it can assess the physicochemical properties of the membrane by utilizing diverse fluorescence-based analytical techniques. As an example, we have demonstrated the application of the FRAP technique to the evaluation of the lipid lateral mobility within the adsorbed planar bilayer membrane. Though the necessity to label the sample with a fluorophore is an obvious drawback, the amount of fluorescence marker can be minimized because of the superior efficiency of surface plasmon excitation. In this study, we used the fluorescence marker (DiD) in the ratio of 1:10,000 with respect to egg-PC molecules, but the ratio could be further reduced with more efficient optical detection systems.

Finally, the development of two-dimensional analysis by SPR-SPFS is described. Fluorescence microscopy has been a major analytical technique for studying planar bilayers on solid substrates. There are a number of variations of fluorescence microscopy, including total internal reflection fluorescence (13,44), fluorescence interference contrast microscopy (45,46), and fluorescence resonance energy transfer (47). They have been providing very specific and detailed information on the topography and physicochemical properties of adsorbed membranes. Therefore, application of the microscopic imaging technique is an important extension for the currently developed analytical approach (SPR-SPFS imaging). Although SPR-SPFS has lesser resolutions compared with AFM or other optical microscopic techniques, simultaneous mapping of the thickness and fluorescence intensities should greatly enhance the obtained information that is useful for diverse applications including ligand-receptor binding assays. Parallel observation of spatially differentiated model cellular membranes (e.g., micropatterned lipid bilayer membrane arrays) should be especially valuable for technological applications such as high-throughput screening.

CONCLUSION AND PERSPECTIVES

We have demonstrated that combined SPR-SFPS is an effective tool for the monitoring of vesicle fusion processes and the physicochemical evaluation of substrate-supported biomimetic membranes. SPR determines the thickness of adsorbed lipid materials in the subnanometer precision, whereas SPFS provides information related to the topography and physicochemical properties of the membrane. As shown by the example of FRAP measurements, various fluorescence-based analytical techniques can be readily combined with SPR-SPFS. Furthermore, the technique has the possibility to be integrated into a microscopic imaging system, enabling parallel analyses of arrays of model cellular membranes. On account of these features, we envisage that SPR-SPFS has the potential for becoming a new standard detection tool for membrane-based biochips and sensors.

K.T. thanks Prof. Dr. W. Knoll and Mr. A. Scheller of Max-Planck-Institute for Polymer Research for their help in constructing the SPFS setup. We thank Dr. J. Nishii, Dr. G. Choi, and Dr. T. Mihara of the National Institute of Advanced Industrial Science for allowing us to use their sputter machines.

This work was supported in part by Promotion Budget for Science and Technology (National Institute of Advanced Industrial Science Upbringing of Talent in Nanobiotechnology Course) from the Ministry of Education, Science, Culture, and Sports and by a Grant-in-Aid for scientific research from the Japan Society for the Promotion of Science.

REFERENCES

1. Sackmann, E. 1996. Supported membranes: scientific and practical applications. *Science*. 271:43–48.
2. Brian, A. A., and H. M. McConnell. 1984. Allogeneic stimulation of cytotoxic T cells by supported planar membranes. *Proc. Natl. Acad. Sci. USA*. 81:6159–6163.
3. Grakoui, A., S. K. Bromley, C. Sumen, M. M. Davis, A. S. Shaw, P. M. Allen, and M. L. Dustin. 1999. The immunological synapse: a molecular machine controlling T-cell activation. *Science*. 285:221–227.
4. Groves, J. T., and M. L. Dustin. 2003. Supported planar bilayers in studies on immune cell adhesion and communication. *J. Immunol. Methods*. 278:19–32.
5. Kloboucek, A., A. Behrisch, J. Faix, and E. Sackmann. 1999. Adhesion-induced receptor segregation and adhesion plaque formation: a model membrane study. *Biophys. J*. 77:2311–2328.
6. Sivasankar, S., B. Gumbiner, and D. Leckband. 2001. Direct measurements of multiple adhesive alignments and unbinding trajectories between cadherin extracellular domains. *Biophys. J*. 80:1758–1768.
7. Salafsky, J., J. T. Groves, and S. G. Boxer. 1996. Architecture and function of membrane proteins in planar supported bilayers: a study with photosynthetic reaction centers. *Biochemistry*. 35:14773–14781.
8. Bunjes, N., E. K. Schmidt, A. Jonczyk, F. Rippmann, D. Beyer, H. Ringsdorf, P. Gräber, W. Knoll, and R. Naumann. 1997. Thiopeptide-supported lipid layers on solid substrates. *Langmuir*. 13:6188–6194.
9. Wagner, M. L., and L. K. Tamm. 2000. Tethered polymer-supported planar lipid bilayers for reconstruction of integral membrane proteins: silane-polyethyleneglycol-lipid as a cushion and covalent linker. *Biophys. J*. 79:1400–1414.
10. Tanaka, M., A. P. Wong, F. Rehfeldt, M. Tutus, and S. Kauffman. 2004. Selective deposition of native cell membranes on biocompatible micropatterns. *J. Am. Chem. Soc*. 126:3257–3260.

11. Giess, F., M. G. Friedrich, J. Heberle, R. L. Naumann, and W. Knoll. 2004. The protein-tethered lipid bilayer: a novel mimic of the biological membrane. *Biophys. J.* 87:3213–3220.
12. Nollert, P., H. Kiefer, and F. Jähnig. 1995. Lipid vesicle adsorption versus formation of planar bilayers on solid surfaces. *Biophys. J.* 69: 1447–1455.
13. Kalb, E., S. Frey, and L. K. Tamm. 1992. Formation of supported planar bilayers by fusion of vesicles to supported phospholipid monolayers. *Biochim. Biophys. Acta.* 1103:307–316.
14. Rädler, J., H. Strey, and E. Sackmann. 1995. Phenomenology and kinetics of lipid bilayer spreading on hydrophilic surfaces. *Langmuir.* 11:4539–4548.
15. Steinem, C., A. Janshoff, W.-P. Ulrich, M. Sieber, and H.-J. Galla. 1996. Impedance analysis of supported lipid bilayer membranes: a scrutiny of different preparation techniques. *Biochim. Biophys. Acta.* 1279:169–180.
16. Williams, L. M., S. D. Evans, T. M. Flynn, A. Marsh, P. F. Knowles, R. J. Bushby, and N. Boden. 1997. Kinetics of the unrolling of small unilamellar phospholipid vesicles onto self-assembled monolayers. *Langmuir.* 13:751–757.
17. Cooper, M. A., A. C. Try, J. Carroll, D. J. Ellar, and D. H. Williams. 1998. Surface plasmon resonance analysis at a supported lipid monolayer. *Biochim. Biophys. Acta.* 1373:101–111.
18. Benes, M., D. Billy, A. Benda, H. Speijer, M. Hof, and W. T. Hermens. 2004. Surface-dependent transitions during self-assembly of phospholipid membranes on mica, silica, and glass. *Langmuir.* 20:10129–10137.
19. Keller, C. A., and B. Kasemo. 1998. Surface specific kinetics of lipid vesicle adsorption measured with a quartz crystal microbalance. *Biophys. J.* 75:1397–1402.
20. Reimhult, E., F. Höök, and B. Kasemo. 2002. Vesicle adsorption on SiO_2 and TiO_2: dependence on vesicle size. *J. Chem. Phys.* 117: 7401–7404.
21. Richter, R., A. Mukhopadhyay, and A. Brisson. 2003. Pathways of lipid vesicle deposition on solid surfaces: a combined QCM-D and AFM study. *Biophys. J.* 85:3035–3047.
22. Reviakine, I., and A. Brisson. 2000. Formation of supported phospholipid bilayers from unilamellar vesicles investigated by atomic force microscopy. *Langmuir.* 16:1806–1815.
23. Muresan, A. S., and K. Y. C. Lee. 2001. Shape evolution of lipid bilayer patches adsorbed on mica: atomic force microscopy study. *J. Phys. Chem. B.* 105:852–855.
24. Schönherr, H., J. M. Johnson, P. Lenz, C. W. Frank, and S. G. Boxer. 2004. Vesicle adsorption and lipid bilayer formation on glass studied by atomic force microscopy. *Langmuir.* 20:11600–11606.
25. Liebermann, T., and W. Knoll. 2000. Surface-plasmon field-enhanced fluorescence spectroscopy. *Colloid. Surface. A.* 177:115–130.
26. Liebermann, T., W. Knoll, P. Sluka, and R. Herrmann. 2000. Complement hybridization from solution to surface-attached probe-oligonucleotides observed by surface-plasmon-field-enhanced fluorescence spectroscopy. *Colloid. Surface. A.* 169:337–350.
27. Knoll, W. 1998. Interfaces and thin film as seen by bound electromagnetic waves. *Annu. Rev. Phys. Chem.* 49:569–638.
28. Tawa, K., and W. Knoll. 2004. Mismatching base-pair dependence of the kinetics of DNA-DNA hybridization studied by surface plasmon fluorescence spectroscopy. *Nucleic Acids Res.* 32:2372–2377.
29. Huang, C., and T. E. Thompson. 1965. Properties of lipid bilayer membranes separating two aqueous phases: determination of membrane thickness. *J. Mol. Biol.* 13:183–193.
30. Ma, C., M. P. Srinivasan, A. J. Waring, R. I. Lehrer, M. L. Longo, and P. Stroeve. 2003. Supported lipid bilayers lifted from the substrate by layer-by-layer polyion cushions on self-assembled monolayers. *Colloid. Surface. B.* 28:319–329.
31. Chance, R. R., A. Prock, and R. Silbey. 1978. Molecular fluorescence and energy transfer near interfaces. *Adv. Chem. Phys.* 37:1–65.
32. Rossetti, R., and L. E. Nrus. 1982. Time resolved energy transfer from electronically excited $^3B_{3u}$ pyrazine molecules to planar Ag and Au surfaces. *J. Chem. Phys.* 76:1146–1149.
33. Zhang, Z.-J., A. L. Verma, N. Tamai, K. Nakashima, M. Yoneyama, K. Iriyama, and Y. Ozaki. 1998. Excitation energy transfer in Langmuir-Blodgett films of 5-(4-Noctadecylpyridyl)-10,15,20- tri-p-tolylporphyrin on gold-evaporated glass substrates studied by time-resolved fluorescence spectroscopy. *Thin Solid Films.* 333:1–4.
34. Edmiston, P. L., L. E. Lee, L. L. Wood, and S. S. Saavedra. 1995. Dipole orientation distributions in Langmuir-Blodgett films by planar waveguide linear dichroism and fluorescence anisotropy. *J. Phys. Chem.* 100:775–784.
35. Castanho, M. A. R. B., S. Lopes, and M. Fernandes. 2003. Using UV-Vis. linear dichroism to study the orientation of molecular probes and biomolecules in lipidic membranes. *Spectroscopy.* 17:377–398.
36. Kawski, A., A. Kubicki, B. Kukliliski, and I. Gryczytiski. 1993. Unusual absorption and fluorescence properties of l,6-diphenyl-l,3,5-hexatriene in poly(viny1 alcohol) film. *J. Photochem. Photobiol. A.* 71:161–167.
37. Sims, P. J., A. S. Waggoner, C.-H. Wang, and J. F. Hoffman. 1974. Studies on the mechanism by which cyanine dyes measure membrane potential in red blood cells and phosphatidylcholine vesicles. *Biochemistry.* 13:3315–3330.
38. Krieg, M., M. B. Srichai, and R. W. Redmond. 1993. Photophysical properties of 3,3′-dialkylthiocarbocyanine dyes in organized media: unilamellar liposomes and thin polymer films. *Biochim. Biophys. Acta.* 1151:168–174.
39. Axelrod, D., D. E. Koppel, J. Schlessinger, E. Elson, and W. W. Webb. 1976. Mobility measurement by analysis of fluorescence photobleaching recovery kinetics. *Biophys. J.* 16:1055–1069.
40. Soumpasis, D. M. 1983. Theoretical analysis of fluorescence photobleaching recovery experiments. *Biophys. J.* 41:95–97.
41. Richter, R. P., and A. Brisson. 2005. Following the formation of supported lipid bilayers on mica: a study combining AFM, QCM-D, and ellipsometry. *Biophys. J.* 88:3422–3433.
42. Keller, C. A., K. Glasmästar, V. P. Zhdanov, and B. Kasemo. 2000. Formation of supported membranes from vesicles. *Phys. Rev. Lett.* 84: 5443–5446.
43. Reimhult, E., C. Larsson, B. Kasemo, and F. Höök. 2004. Simultaneous surface plasmon resonance and quartz crystal microbalance with dissipation monitoring measurements of biomolecular adsorption events involving structural transformations and variations in coupled water. *Anal. Chem.* 76:7211–7220.
44. Johnson, J. M., T. Ha, S. Chu, and S. G. Boxer. 2002. Early steps of supported bilayer formation probed by single vesicle fluorescence assays. *Biophys. J.* 83:3371–3379.
45. Braun, D., and P. Fromherz. 1998. Fluorescence interferometry of neuronal cell adhesion on microstructured silicon. *Phys. Rev. Lett.* 81: 5241–5244.
46. Kiessling, V., and L. K. Tamm. 2003. Measuring distances in supported bilayers by fluorescence interference-contrast microscopy: polymer supports and SNARE proteins. *Biophys. J.* 84:408–418.
47. Wong, A. P., and J. T. Groves. 2002. Molecular topography imaging by intermembrane fluorescence resonance energy transfer. *Proc. Natl. Acad. Sci. USA.* 99:14147–14152.